



Research Paper

On Designing of Membrane Thickness and Thermal Conductivity for Large Scale Membrane Distillation Modules

A. Ali^{1,*}, C.A. Quist-Jensen^{1,2}, F. Macedonio^{1,2}, E. Drioli^{1,2,3,4}¹ Institute on Membrane Technology (ITM-CNR), National Research Council, c/o University of Calabria, Cubo 17C, Via Pietro Bucci, 87036 Rende CS, Italy² University of Calabria - Department of Environmental and Chemical Engineering, Rende, Italy³ Hanyang University, WCU Energy Engineering Department, Seoul 133-791, S. Korea⁴ Center of Excellence in Desalination Technology, King Abdulaziz University, Jeddah, Saudi Arabia

ARTICLE INFO

Received 2016-01-20
 Revised 2016-02-10
 Accepted 2016-02-13
 Available online 2016-02-13

KEYWORDS

Membrane distillation (MD)
 Crystallization
 Thickness
 Thermal conductivity
 Length

HIGHLIGHTS

- Membrane thickness, thermal conductivity and fiber length mutually affect MD process.
- Any of these parameters cannot be optimized without considering the other two.
- Optimum length can be tuned by varying membrane thickness and/or thermal conductivity.

ABSTRACT

Membrane distillation has the potential to concentrate solutions to their saturation level, thus offering the possibility to recover valuable salts from the solutions. The process performance and stability, however, is strongly dependent upon the features of membranes applied. In addition, several other parameters, membrane thickness and thermal conductivity significantly affect the process performance. These parameters are of fundamental importance in the selection of optimum module length due to their influence on temperature and flux profiles along the fiber. In the current study, the experimental data from a lab-scale membrane distillation plant has been modeled to analyze the interrelated effect of membrane thickness, thermal conductivity and module length on process performance. It has been observed that flux initially improves by decreasing the membrane thickness followed by a decrease and ultimately negative value. For any given fiber length and thickness, the flux can be greatly improved by decreasing the membrane-conductivity. The length that corresponds to the highest flux and the maximum fiber length ensuring a positive flux have been identified as a function of membrane thickness and thermal conductivity.

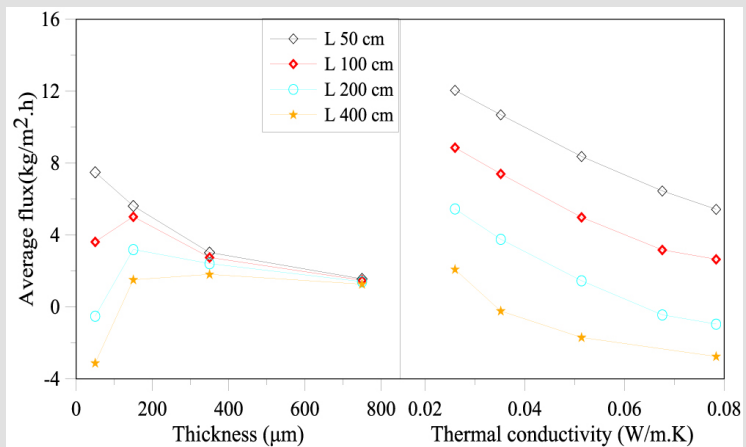
© 2016 MPRL. All rights reserved.

1. Introduction

Growing energy demands, depleting raw materials, water scarcity and environment issues are compelling the process industry to look towards innovative solutions. Emerging membrane operations such as membrane distillation (MD) can play an important role in this context. In MD, the volatiles are transported through a microporous hydrophobic membrane under

the vapor pressure gradient applied through temperature difference across the membrane [1]. The process has the potential to treat high-concentrated solutions and thus offers the possibility to recover valuable components from various liquid streams. MD has been investigated intensively at the lab-scale for desalination due to its unique advantages including the possibility to operate with waste grade heat, minor effect of concentration on process

GRAPHICAL ABSTRACT



performance and theoretically 100% rejection of all non-volatiles. The major targeted areas for research in MD include the development of specific membranes, understanding and improvement of transport phenomena and novel applications for various separations [2,3]. The progress in the field has recently resulted in manufacturing and testing of pilot scale units in various parts of the world [4,5,6]. These units aim to test the techno-economic feasibility of the process for its large scale applications when integrated with other processes [7,8]. Such advancements provoke the need to fabricate large scale modules and understanding the performance of these modules as a function of membrane characteristics.

One of the most interesting applications of MD is the treatment of concentrated brine to increase the recovery factor and eventually to achieve crystallization. Technical feasibility of this application at lab-scale has been demonstrated in several studies [9–11]. To realize the crystallization through MD, the solutions have to be treated to the saturation level. For successful application of MD-based crystallization (commonly known as membrane crystallization), better understanding of the correlation between membrane characteristics and process performance is essential. One of the possibilities to tune the process performance can be based upon changing the membrane thickness and thermal conductivity. A few studies have addressed the optimum membrane thickness for MD applications. Wu et al. [12] have reported an optimum membrane thickness of 13 microns for treatment of 10% saline solution that increases to 21 microns at 20% salinity. Based on the flux and energy efficiency, Martinez and Rodriguez [13] have also indicated a critical membrane thickness below which the negative effect prevails the positive outcomes. Eykens et al. [14] have reported that optimum membrane thickness varies with operating conditions and membrane characteristics and ranges from 2 to 739 microns. However, these studies are performed without interrelating membrane thickness and thermal conductivity with module length which is crucial for large scale applications.

For lab-scale membrane crystallization applications, feed temperature at the module inlet is generally set to 10-15 °C more than the feed tank temperature [15]. Besides mitigating the scaling at membrane surface, high temperature provided at the module inlet ensures the supply of sufficient driving force required to maintain a positive flux. However, when high-concentrated feed flows in modules with practically long length, the osmotic pressure of feed at such high concentration might prevail the thermal effect (due to large temperature drops along the module) giving rise to undesired negative flux. For the salts with positive solubility with temperature, large temperature drops can also increase the probability of precipitation at the membrane surface and within the feed channel. Furthermore, the energy efficiency of the process is a strong function of temperature profiles along the module. In this context, membrane thickness and thermal conductivity controlling the heat and mass transfer can be significantly important to ensure the positive flux, to define the optimum module length and to ensure a precipitation-free operation. This study describes the performance of membrane distillation as a function of membrane thickness for various membrane lengths and thermal conductivities for a high-concentrated solution.

2. Materials and methods

2.1. MD tests

The data for MD experiments reported in our previous work [16] has been modeled in the current study. The tests were performed on produced water with initial concentration of 248 g/L. The main dissolved solid was sodium chloride. Lab and semi pilot-scale experiments were carried out by using commercial Accurel PP-S 6/2 and lab-made PVDF hollow fiber membranes. The detailed solution composition, operating conditions and membrane characteristics can be found in the same reference (see [16]).

To avoid salt precipitation at the membrane surface and for better process control, membrane crystallization is normally performed at relatively low solution temperatures (30-55 °C) [11,16,17]. Therefore, modeling analysis in the current study has been carried out by assuming the feed and permeate temperatures at module inlet equal to 50 °C and 20 °C, respectively. It was observed in the previous study that the scaling can be avoided by carefully controlling the temperature of feed tank below the feed temperature at module inlet [16]. Therefore, the effect of scaling has been neglected in the current study. Due to the decrease in driving force with solution concentration, the bottleneck of the process is near the saturated- solution concentration making the process most interesting to study at this point. Due to this reason, theoretical analysis in the current study has been carried out at near saturated concentration (~340 g/L). Feed and permeate velocities have been considered equal for theoretical analysis and both the streams are assumed in countercurrent configuration.

2.2. Modeling procedure

The basic modeling procedure applied for the current study has been explained in detail in a previous publication [16], therefore, the procedure has been described only briefly here. The flux in MD can be described by using the following correlation:

$$J = B(P_{fm} - P_{pm}) \quad (1)$$

where P_{fm} and P_{pm} are vapor pressures of feed and permeate, respectively, at the corresponding membrane surface temperatures T_{fm} and T_{pm} . To account for the effect of salt on vapor pressure, Yun's method [18] has been applied. For membrane characteristics parameter B , the combined Knudsen and molecular diffusion model has been applied due to close proximity of membrane pore size and mean free path of water vapors under the conditions applied in the current study.

The appropriate heat transfer coefficient has been calculated according to the procedure described in [16]. On the basis of feed and permeate temperatures and heat transfer coefficient, the temperatures at the membrane surface have been calculated by using the following correlations [19].

$$T_{fm} = T_f - (T_f - T_p) \frac{1/h_f}{1/h_v + h_c + 1/h_p + 1/h_f} \quad (2)$$

$$T_{pm} = T_p + (T_f - T_p) \frac{1/h_p}{1/h_v + h_c + 1/h_p + 1/h_f} \quad (3)$$

where h_f and h_p represent the heat transfer coefficients on feed and permeate sides, respectively, while h_v and h_c are the vapor and membrane heat transfer coefficients.

To obtain temperature and flux profiles along the fiber in the current study, the membrane has been divided into small elements, each having a length L such that the total number of elements is L/L , where L represents the total membrane length. Heat and mass balance on each cell on feed and permeate streams have been applied. Difference in energy at the entrance and exit of the cell on the feed side is transported through the membrane via conduction and convection [20]:

$$\dot{m}_f CpT \Big|_i - \dot{m}_f CpT \Big|_{i+1} = \frac{K_m}{\delta} (T_{fm} - T_{pm}) dA + J \Delta H_v dA \quad (4)$$

$$T \Big|_{i+1} = \frac{\dot{m}_f CpT \Big|_i - \left(\frac{K_m}{\delta} (T_{fm} - T_{pm}) dA + J \Delta H_v dA \right)}{\dot{m}_f Cp \Big|_{i+1}} \quad (5)$$

Similarly, the permeate temperature at the boundary of the next cell can be determined by using the following correlation:

$$T \Big|_{i+1} = \frac{\dot{m}_p CpT \Big|_i - \left(\frac{K_m}{\delta} (T_{fm} - T_{pm}) dA + J \Delta H_v dA \right)}{\dot{m}_p Cp \Big|_{i+1}} \quad (6)$$

On the basis of flux and surface and bulk temperatures, various resistances to mass transfer can be calculated by using the following correlations [21]:

$$R_f = \frac{P_f - P_{fm}}{J} \quad (7)$$

$$R_p = \frac{P_{pm} - P_p}{J} \quad (8)$$

$$R_m = \frac{P_{fm} - P_{pm}}{J} \quad (9)$$

where R_m , R_f and R_p represent the membrane, feed and permeate side boundary layer resistance, respectively.

3. Results and discussions

3.1. Model validation

The model was validated by comparing the predicted flux with its corresponding experimental values at 35, 45 and 55 °C provided in [16] for PP and PVDF membranes. Experimental and theoretical flux calculated by

using the heat transfer correlation proposed by Gryta and Tomaszewska [22] have been provided in Figure 1. The figure shows an excellent agreement between experimental and theoretical values. The decrease in flux with concentration can be ascribed to the corresponding decrease in vapor pressure of feed due to an increase in solution concentration. Relatively higher flux exhibited by the PVDF membrane can be attributed to its more porous structure and lower thickness than the PP membrane as explained in [16].

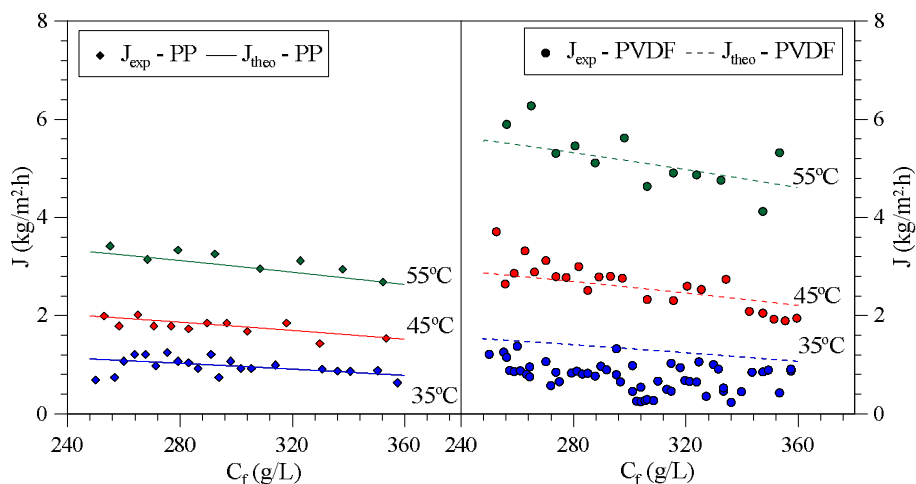


Fig. 1. Experimental and theoretical flux as function of solution concentration for PP Accurel and PVDF membranes under various feed inlet temperatures

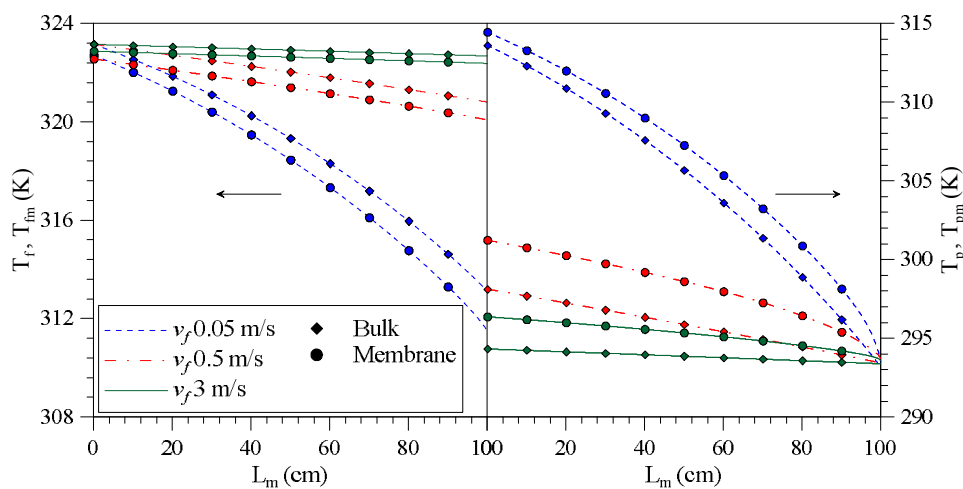


Fig. 2. Variation of bulk and membrane surface temperatures along the fiber for various values of v_f for membrane thickness of 450 μm .

3.2. Selection of appropriate feed velocity

Temperature profiles at various locations along 1m long fiber for different feed velocities have been shown in Figure 2. It is clear from the figure that the maximum temperature polarization and temperature drop along the fiber takes place for the minimum feed velocity of 0.05 m/s in accordance with what has been observed in other studies [23,24]. Low feed velocity increases the contact time of feed and permeate streams and limits the mixing of fluid present at the membrane interface and in the bulk. The former contributes to the large temperature drops along the module while the later encourages temperature polarization. As a result, the minimum temperature polarization and temperature drop along the module have been observed for the highest feed velocity while these effects are the maximum for the lowest feed velocity. A similar trend has been observed for the permeate side. The maximum temperature increase (temperature difference between outlet and inlet of the module) has been observed for the minimum permeate velocity. Similar to the feed side, the temperature profiles start to be uninform along the fiber length by increasing the permeate flow rate. However, temperature polarization on the permeate side is the maximum for v_f of 0.5 m/s (and not for the minimum permeate velocity of 0.05 m/s). It is well recognized that

thermal polarization increases with stream temperature and reduces with velocity [23–25]. By increasing the flow rate, the feed temperature starts to improve and be uniform along the module. This ensures high heat transfer from the feed to permeate side, thus widening the difference between surface and bulk temperature on the permeate side (see for v_f 0.5 m/s). With a further increase in velocity, the temperature along the fiber improves relatively less and improved hydrodynamics reduce thermal polarization. The minimum thermal polarization on the permeate side observed at the start of the fiber (100 cm) is due to the entrance effect that induce additional turbulence.

Although working at high v_f reduces thermal polarization and temperature drop along the fiber, it may cause large pressure drops along the membrane modules leading towards pore wetting. Moreover, it may reduce overall membrane life time due to high shear stress acting at the membrane surface. Due to this reason, the main investigations in this study have been carried out at v_f of 1 m/s where temperature polarization and temperature drop along the module are not very significant (see Figure 2).

The effect of membrane thickness on temperature profiles for membranes with various thicknesses at v_f of 1 m/s for 1 m long fiber has been shown in Figure 3. It is clear from the figure that the thinnest membrane exhibits the maximum thermal polarization and bulk temperature variations along the

fiber on both permeate and feed sides. The average temperature polarization on feed and permeate sides for the 30 μm thick membrane is ~2 and ~8 K, respectively, while the corresponding values for the 750 μm thick membrane are 0.3 and 1.4 K, respectively. Thin membranes favor the conductive and convective heat transfer across the membrane wall that increases temperature polarization and temperature drop along the fiber. Large feed side temperature polarization observed near the end (100 cm) of the thinnest membrane is due to the corresponding low permeate temperature due to the entrance effect that induces high driving force at the corresponding point giving rise to high thermal polarization.

The corresponding flux for membranes with selected thicknesses has been illustrated in Figure 4. The thinnest membrane exhibits the negative flux in the first portion of the fiber (Lm < ~60 cm). It is clear from Figure 3 that the effective temperature gradient (T_{fm} - T_{pm}) across the membrane reduces with a decrease in membrane thickness. Although the temperature gradient (T_{fm} - T_{pm}) at any point along the fiber for all the membranes is positive, the

solution concentration suppresses the vapor pressure on the feed side. Assuming equal feed and permeate temperatures (323 K), the vapor pressure on the feed side is ~6000 Pa less than the permeate side. For the 450 μm thick membrane, keeping the permeate temperature and other conditions constant, feed temperature should be a minimum 10 °C greater than permeate temperature to overcome this suppression. As shown in Figure 3, interfacial permeate temperature increases suddenly for the 30 μm thick membrane after coming in contact with feed stream. Due to this increase and associated decrease in the corresponding feed temperature, the effective temperature gradient after a certain distance from the permeate entrance drops below the threshold value required to induce positive flux. Thus flux in the later portion of the fiber (~60 to 0 cm) becomes negative due to the corresponding negative net driving force (vapor pressure difference ΔP) shown on the right in Figure 4. In case of thicker membranes, the effective temperature gradient (and therefore vapor pressure difference) is high enough to overcome the concentration effects, thus giving a positive flux.

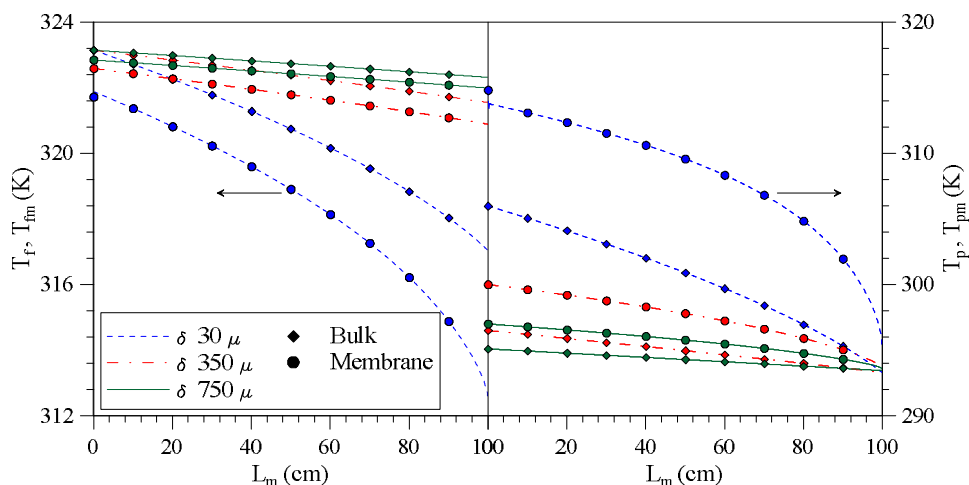


Fig. 3. Effect of membrane thickness on temperature profiles for v_f of 1 m/s.

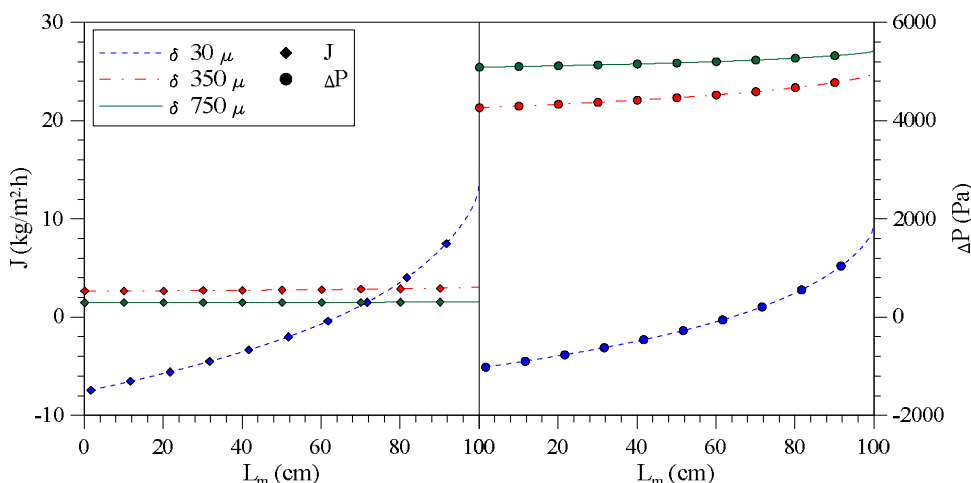


Fig. 4. Flux at various points along the fiber for membranes with different thicknesses at v_f 1 m/s.

The energy efficiency and flux averaged over module length (J_{av}) for the 1 m long module have been shown in Figure 5. The average flux improves greatly by an initial increase in membrane thickness followed by a steady decrease. This trend is consistent with what has been reported in other studies [12,26]. For the very thin membrane, the mass transfer is governed by the boundary layer resistance. By increasing the membrane thickness, thermal polarization on both sides of the membrane reduces. However, after a certain membrane thickness, the membrane itself starts to control the mass transfer and therefore, flux shows a decreasing trend with an increase in membrane thickness. The figure also indicates an initial abrupt increase in energy efficiency at 100 μm thickness followed by slight dependence on membrane thickness. The former behavior is associated with rapid initial increase in flux

with membrane thickness as shown in the same figure. By further increasing the membrane thickness, the flux decreases slightly, however, the heat transfer coefficient of the membrane decreases relatively more and therefore, energy efficiency slightly improves.

3.3. Effect of module length

Module length is an important parameter from a practical point of view. The small modules offer low productivity, do not utilize the heat contained within the stream in an efficient way and may not be techno-economically viable to assemble in an element. Average flux as a function of module length for various membrane thicknesses has been shown in Figure 6. The figure

illustrates that small fibers with low thicknesses exhibit very high average flux. For instance, the average flux for the 50 cm long fiber having a thickness of 50 μm is ~ 3 times higher than the same fiber but with a thickness of 750 μm . However, thin fibers show a rapid decrease in average flux with an increase in length and for long lengths, the flux becomes negative in the later portion of the fiber. For instance, 50 μm thick fibers having length > 190 cm exhibit negative flux. Thick fibers, on the other hand, show stable flux for all module lengths. As explained in Figure 3, thin fiber rapidly loses the thermal energy contained within the feed through conduction and convection through the membrane, and consequently, the temperature along the fiber drops quickly. While in the initial portion of the fiber, the temperature would be sufficient to generate flux, in the later portion, the temperature would not be enough to keep a positive driving force. The net effects can result into an overall negative flux. The thicker fibers, on the other hand, reduce thermal losses through conduction and convection (due to less flux), giving rise to relatively uniform driving force and flux all along the fiber.

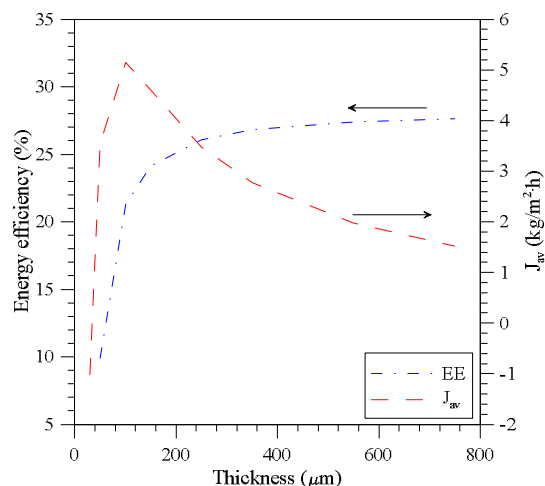


Fig. 5. Energy efficiency (EE) and average flux as function of membrane thickness for 1 m long module.

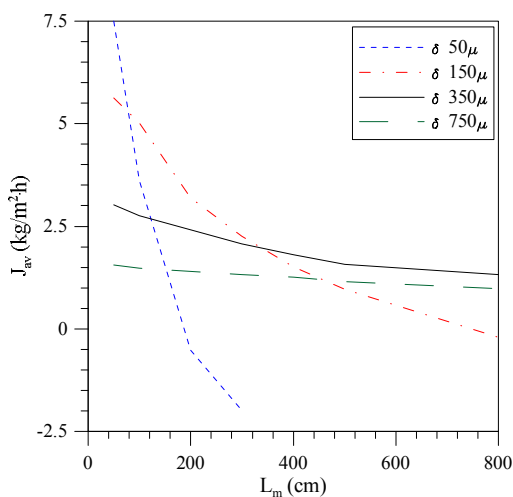


Fig. 6. Flux averaged over fiber lengths for membranes with different thicknesses at v_f 1 m/s.

The flux averaged over lengths for fibers with various thicknesses is shown in Figure 7. The figure indicates that the difference among the fluxes for fibers with different lengths is the most prominent at small membrane thicknesses and converges at high thicknesses. Also, the membrane thickness corresponding to the highest flux increases with fiber length. For instance, a 20 cm long fiber exhibits the highest flux at a thickness of ~ 40 μm and this value shifts to ~ 150 μm for 300 cm long fiber. Similarly, the minimum thickness required to maintain a positive flux, is a function of module length and changes from ~ 15 to 85 μm when length is changed from 20 to 300 cm under the conditions considered in the current study. This behavior can be attributed to the corresponding resistances shown in Figure 8. Flux of the system is determined by the membrane resistance and sum of feed and

permeate side resistances ($R_f + R_p$) shown in Figure 8. As shown in the figure, the main contribution to the overall resistance comes from the boundary layer resistances $R_f + R_p$, as the thin membrane itself offers much less resistance to mass transfer but transfers more heat giving rise to high thermal polarization [27]. However, by increasing the membrane thickness, the contribution of membrane resistances to mass transfer increases and that of the boundary layer decreases. The thickness where the sum of these two contributions is the minimum corresponds to the highest flux shown in Figure 7. The minimum however, depends upon the temperature profiles within the fiber, and therefore, is different for different fiber lengths as shown in Figure 8 for a 20 and 300 cm long fiber.

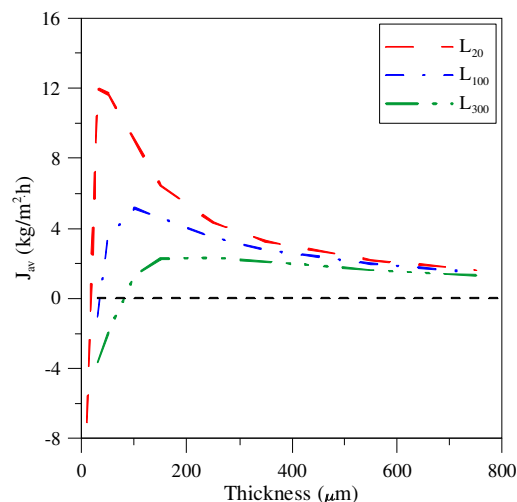


Fig. 7. Average flux as function of membrane thickness for various fiber lengths. The lowest horizontal line corresponds to zero flux.

3.4. Effect of membrane conductivity

Thermal conductivity controls the heat flowing through the membrane matrix via conduction and therefore temperature profiles within the fiber. The effect of thermal conductivity on the trans-membrane flux for various module lengths has been shown in Figure 9. The lowest value of thermal conductivity (0.026 W/m.K) considered in the current study was inspired from the conductivity value of aerogel ceramic membranes recently developed for MD applications [28]. All other membrane features including overall porosity, mean pore size and tortuosity factor have been considered constant. The figure reveals that the membrane with the lowest thermal conductivity shows the highest flux at any given length. For fiber length of 50 cm, $\sim 90\%$ increase in flux can be achieved by decreasing the thermal conductivity from 0.08 to 0.026 W/m.K. The corresponding increase for longer fibers is even higher. Similar to the membrane thickness, high flux observed for the membranes with less conductivity can be associated with their capability to conduct less heat along the fiber. Relatively lower loss of heat ensures a high temperature along the fiber, giving a better overall flux. The results described in Figure 9 provide an interesting way to improve the membrane flux and the maximum effective module length by lowering the conductivity of the membrane. For a membrane with 50 μm thickness and thermal conductivity of ~ 0.07 W/m.K, the flux would become negative for module lengths exceeding ~ 2 m, however, by decreasing the thermal conductivity the module lengths with positive flux of more than 4 m are possible to achieve. This aspect can be of significant importance in designing the modules with optimized length.

The effect of membrane thickness on length exhibiting the maximum flux for various values of membrane conductivity has been illustrated in Figure 10. Lowering the thermal conductivity affects the temperature profile in a manner similar to that observed for an increase in thickness shown in Figure 3. However, contrary to the thickness, it does not increase the resistance to mass transport. A fiber with high conductivity encourages more heat transfer via conduction through its wall. Consequently, the temperature on the feed side decreases rapidly and that on the permeate side increases largely. Therefore, for a given membrane thickness, the maximum driving force is observed somewhere in between the feed and permeate inlets. However, a decrease in thermal conductivity of the fiber ensures a slow increase and decrease of the permeate and feed temperatures, respectively, along the fiber and therefore, the point of maximum flux shifts towards smaller fiber lengths where feed temperature is high.

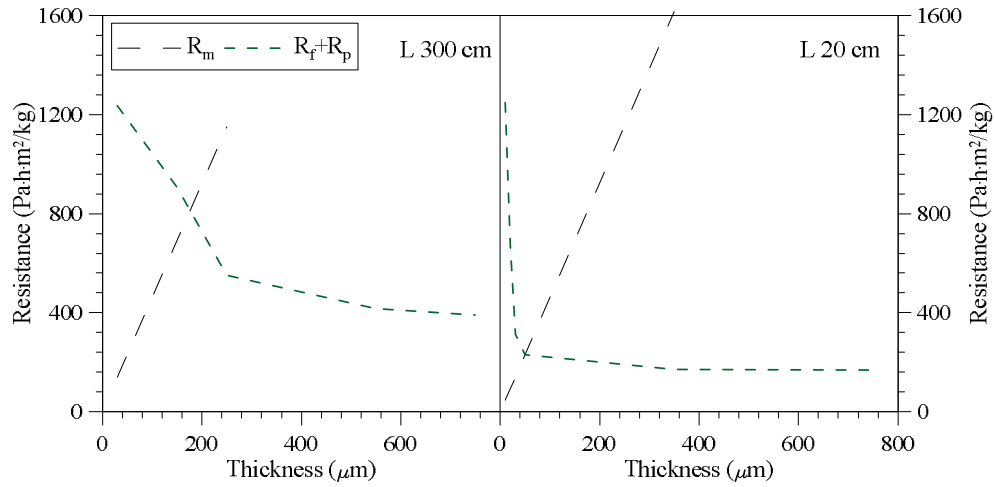


Fig. 8. Resistance analysis as function of membrane thickness for 300 and 20 cm long fibers.

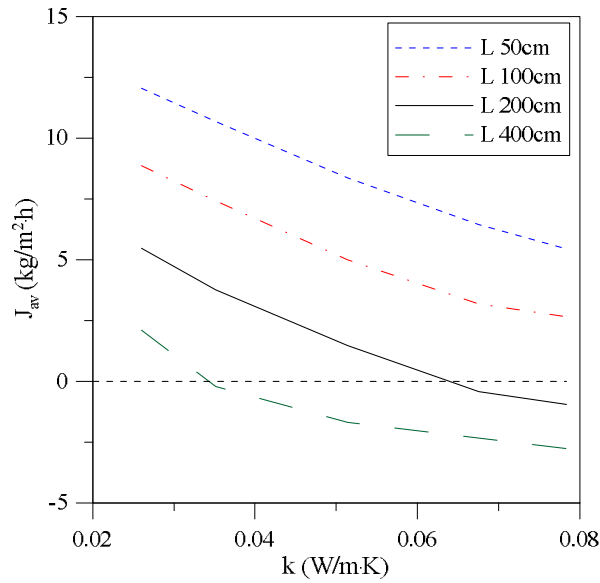


Fig. 9. Flux as function of thermal conductivity for fibers with different lengths for 50 μm thick membrane at v_f 1 m/s.

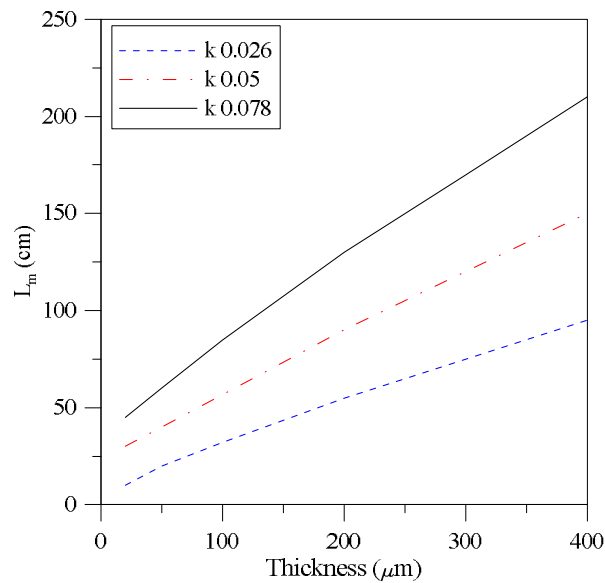


Fig. 10. Module length yielding the maximum flux as function of membrane thickness for various values of membrane conductivity.

4. Conclusions

The performance of the membrane distillation process is strongly influenced by membrane thickness and thermal conductivity. A strong nexus among thickness, thermal conductivity and fiber length governs the process performance and it is not rational to define the optimum value of one of these parameters without considering the others. For an inappropriate combination of membrane thickness, thermal conductivity and length, the osmotic effects may overcome the thermal effects and a negative flux is observed. The membranes with low thickness, long length and high thermal conductivity are more prone to negative flux. To make a module of greater than 2 m length by using a 50 μm thick membrane, thermal conductivity of the membrane must be less than 0.065 W/m.K. The upper limit of thermal conductivity can be increased by increasing the membrane thickness or by decreasing the module length. The optimum membrane thickness varies from 20 to 400 microns when thermal conductivity and module lengths are varied from 0.026 to 0.078 W/m.K and 10 to 210 cm, respectively.

List of symbols

B	Membrane characteristics parameter
C	Concentration (g/L)
h	Heat transfer coefficient (W/ $\text{m}^2\cdot\text{K}$)
J	Flux ($\text{kg}/\text{m}^2\cdot\text{s}$)
k	Thermal conductivity (W/m.k)
L_m	Membrane/module/fiber length (cm)
M	Molecular weight (kg/mol)
P	Vapor pressure (Pa)
T	Temperature (K)
E_E	Energy efficiency (%)
v	Velocity (m/s)

Suffix

a_v	Average
f	Feed
m	Membrane
p	Permeate

Greek symbols

δ	Membrane thickness (μm)
----------	--------------------------------------

References

- [1] A. Alkhdhiri, N. Darwish, N. Hilal, Membrane distillation: A comprehensive review, *Desalination* 287 (2012) 2–18.
- [2] L. Camacho, L. Dumée, J. Zhang, J. Li, M. Duke, J. Gomez, S. Gray, Advances in Membrane Distillation for Water Desalination and Purification Applications, *Water* 5 (2013) 94–196.
- [3] M. Khayet, Membranes and theoretical modeling of membrane distillation: a review, *Adv. Colloid Interface Sci.* 164 (2011) 56–88.
- [4] E. Mendez, Membrane distillation delivers greener clean water, *Filtr. Sep.* 49 (2012) 26–28.
- [5] A. Cha, S. Al-zahrani, M. N. Al-otaibi, C. F. Hoong, T. F. Lai, M. Prabu, Portable and integrated solar-driven desalination system using membrane distillation for arid remote areas in Saudi Arabia, *Desalination* 345 (2014) 36–49.
- [6] A. Jansen, J. Hanemaaijer, J. Assink, E. Van Sonbeek, C. Dotremont, J. Van Madevoort, Pilot plants prove feasibility of a new desalination technique, *Asian Water*, March (2010) 22–26.
- [7] S. Kim, B. S. Oh, M.-H. Hwang, S. Hong, J. H. Kim, S. Lee, I. S. Kim, An ambitious step to the future desalination technology: SEASHERO R&D program (2007–2012), *Appl. Water Sci.* 1 (2011) 11–17.
- [8] M. Kurihara and M. Hanakawa, Mega-ton Water System: Japanese national research and development project on seawater desalination and wastewater reclamation, *Desalination* 308 (2013) 131–137.
- [9] F. Macedonio, L. Katzir, N. Geisma, S. Simone, E. Drioli, J. Gilron, Wind-Aided Intensified evaporation (WAIV) and Membrane Crystallizer (MCR) integrated brackish water desalination process: Advantages and drawbacks, *Desalination* 273 (2011) 127–135.
- [10] W. Li, B. Van der Bruggen, P. Luis, Integration of reverse osmosis and membrane crystallization for sodium sulphate recovery, *Chem. Eng. Process: Process Intensif.* 85 (2014) 57–68.
- [11] F. Macedonio, C. a. Quist-Jensen, O. Al-Harbi, H. Alromaih, S. a. Al-Jlil, F. Al Shabouna, E. Drioli, Thermodynamic modeling of brine and its use in membrane crystallizer, *Desalination* 323 (2013) 83–92.
- [12] H. Yan, R. Wang, R. W. Field, Direct contact membrane distillation: An experimental and analytical investigation of the effect of membrane thickness upon transmembrane flux, *J. Membr. Sci.* 470 (2014) 257–265.
- [13] L. Martinez, J. M. Rodriguez-Maroto, Membrane thickness reduction effects on direct contact membrane distillation performance, *J. Membr. Sci.* 312 (2008) 143–156.
- [14] L. Eykens, I. Hitsov, K. De Sitter, C. Dotremont, L. Pinoy, I. Nopens, Influence of membrane thickness and process conditions on direct contact membrane distillation at different salinities, *J. Membr. Sci.* 498 (2016) 353–364.
- [15] X. Ji, E. Curcio, S. Al, G. Di, E. Fontananova, E. Drioli, Membrane distillation-crystallization of seawater reverse osmosis brines, *Sep. Purif. Technol.* 71 (2010) 76–82.
- [16] A. Ali, C. A. Quist-jensen, F. Macedonio, E. Drioli, Application of Membrane Crystallization for Minerals' Recovery from Produced Water, *Membranes (Basel)* 5 (2015) 772–792.
- [17] C. M. Tun, A. G. Fane, J. T. Matheickal, R. Sheikholeslami, Membrane distillation crystallization of concentrated salts—flux and crystal formation, *J. Membr. Sci.* 257 (2005) 144–155.
- [18] Y. Yun, R. Ma, W. Zhang, A. G. Fane, J. Li, Direct contact membrane distillation mechanism for high concentration NaCl solutions, *Desalination* 188 (2006) 251–262.
- [19] L. Martinez-Diez and M. I. Vazquez-Gonzalez, Temperature and concentration polarization in membrane distillation of aqueous salt solutions, *J. Membr. Sci.* 156 (1999) 265–273.
- [20] J. Zhang, S. Gray, J. Li, Modelling heat and mass transfers in DCMD using compressible membranes, *J. Membr. Sci.* 387–388 (2012) 7–16.
- [21] A. Ali, P. Aimar, E. Drioli, Effect of module design and flow patterns on performance of membrane distillation process, *Chem. Eng. J.* 277 (2015) 368–377.
- [22] M. Gryta, M. Tomaszewska, Heat transport in the membrane distillation process, *J. Membr. Sci.* 144 (1998) 211–222.
- [23] A. Ali, F. Macedonio, E. Drioli, S. Aljlil, O. A. Alharbi, Experimental and theoretical evaluation of temperature polarization phenomenon in direct contact membrane distillation, *Chem. Eng. Res. Des.* 91 (2013) 1966–1977.
- [24] J. Phattaranawik, R. Jiratananon, A. G. Fane, Heat transport and membrane distillation coefficients in direct contact membrane distillation, *J. Membr. Sci.* 212 (2003) 177–193.
- [25] M. Martinez-Diez, L. Vazquez-Gonzalez, Temperature and concentration polarization in membrane distillation of aqueous salt solutions, *J. Membr. Sci.* 156 (1999) 265–273.
- [26] L. Martínez, J. M. Rodríguez-Maroto, Membrane thickness reduction effects on direct contact membrane distillation performance, *J. Membr. Sci.* 312 (2008) 143–156.
- [26] L. Martínez, J. M. Rodríguez-Maroto, Membrane thickness reduction effects on direct contact membrane distillation performance, *J. Membr. Sci.* 312 (2008) 143–156.
- [27] A. M. Alkhaibi, N. Lior, Heat and mass transfer resistance analysis of membrane distillation, *J. Membr. Sci.* 282 (2006) 362–369.
- [28] F. H. K. Tung, C. Ko, C. Chen, A. Huang, Y. Lin, M. Huang, Hydrophobic aerogel membranes for membrane distillation application in desalination: in the 2nd International workshop on membrane distillation and innovating membrane operations in desalination and water reuse, Ravello, Italy, 1–4th July, 2015.